Results from the NASA Automated Nap-of-the-Earth Program

Richard E. Zelenka
Phillip N. Smith
Richard A. Coppenbarger
Chima E. Njaka
Banavar Sridhar
NASA Ames Research Center, Moffett Field, CA

ABSTRACT

Military helicopter Nap-of-the-Earth (NOE) flight represents one of the most demanding low-altitude, near terrain flight operations. In NOE, the pilot is operating at or below tree-top levels, taking maximum advantage of the covertness provided by the terrain and ground features for concealment. Such increased proximity to obstructions places heightened maneuverability requirements on the aircraft and extreme levels of workload on the pilot.

The basic issue being addressed in the NASA Automated Nap-of-the-Earth (ANOE) program is the intelligent use of environmental information such as knowledge of terrain, obstacles, and other external factors to enhance the flight path guidance of the vehicle. This is a major departure over contemporary guidance and control which is predicated on state-feedback of variables such as vehicle attitudes, velocities, and accelerations. Although the immediate program has a military focus, the technological advances inherent for automating NOE flight have great benefit to the operation of a wide class of vehicles such as emergency medical helicopters, conventional and high-speed transports, unmanned aerial vehicles, and planetary vehicles.

This paper summarizes the results to date of the NASA ANOE program in the areas of passive sensors, active sensors, pilot displays, low-altitude manual trajectory guidance, and NOE automatic guidance. Each of these component areas, separately and in various combinations, have been developed and evaluated in piloted, motion-based simulation or through flight test. These evaluations have realized the feasibility of automating the NOE flight mission, and have generated additional spin-off applications of the technologies.

INTRODUCTION

Pilots flying rotorcraft close to the ground in nap-of-the-earth flight are confronted with unique guidance and control tasks such as aircraft concealment, obstacle avoidance, and long-range mission planning. These flight tasks require a high degree of skill and concentration, and can be intensified by low-visibility and high auxiliary workload conditions. Automation in this flight regime is motivated by the desire to reduce pilot workload without compromising pilot confidence and safety.

The objective of the NASA Automated Nap-of-the-Earth program is to develop technology to aid the helicopter pilot during low-altitude and NOE flight through computer and sensor augmentation. The program has focused on three discrete technology areas: 1) processing methods for acquiring terrain and obstacle information from passive and active sensors, 2) the use of stored digital terrain data in conjunction with highly accurate navigation systems for improved low-altitude guidance, and 3) the augmentation or correction of stored digital terrain data through the use of forward-looking sensors and the integration of these sensor data into the flight guidance and control systems in manual and automatic modes.

All three development technology areas goals involve conceptualization, analysis, hardware implementation, and flight test. The first and third technology areas are being conducted on the NASA/Army UH-60 RASCAL (Rotorcraft Aircrew Systems Concepts Airborne Laboratory) test helicopter. The second technology area has been accomplished in joint flight test with the U.S. Army aboard the Army UH-60 STAR (Systems Testbed for Avionics Research) test helicopter. The NASA VMS (Vertical Motion Simulator) facility has been used extensively, in conducting piloted, motion-based high fidelity graphic flight simulations. Because automation in nap-of-the-earth flight is such a revolutionary concept, the piloted evaluation studies

Presented at the American Helicopter Society 52nd Annual Forum, Washington, D.C. June 4-6, 1996.

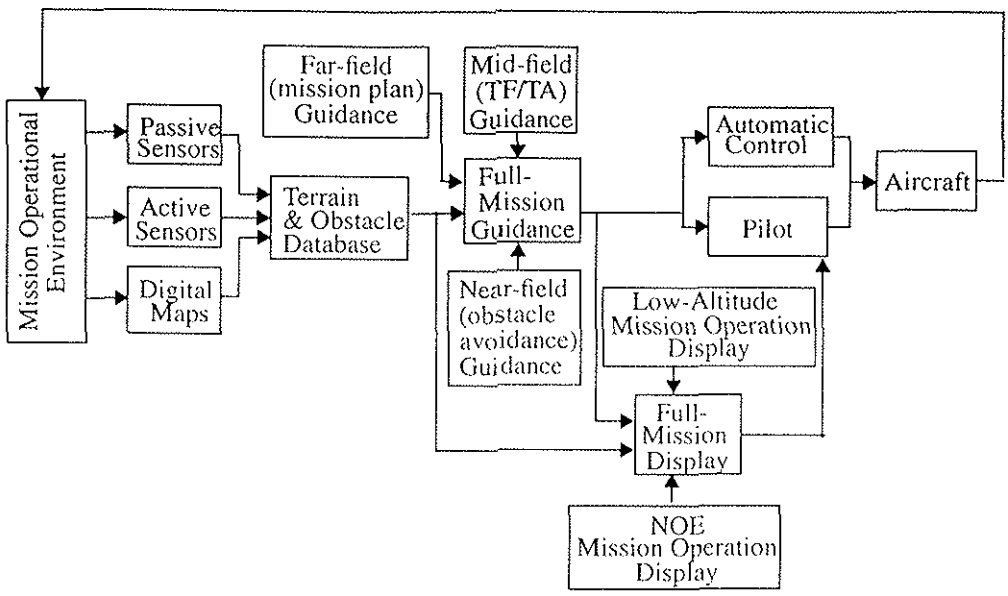

Fig.1. Overall Automated NOE system architecture.

include concepts for low-altitude (above tree-top) as well as NOE (below tree-top) flight. Such aids for low-altitude flight have direct application to certain missions (e.g. military special operations, search and rescue) and offer the potential of being a first step in piloted automation in proximity to terrain.

The NASA ANOE program is composed of the following component technologies:

1) *Passive Sensors:* the use of "pixel-flow" data from television and infrared cameras to detect and extract range and position to objects and terrain. Such sensors offer high update rates and wide field of views without emitting energy.

2) *Active Sensors:* the use of millimeter wave (MMW) radar and laser radar to detect and extract range and position to objects and terrain. Such sensors offer very accurate ranging to objects, fine resolution, and operation in degraded weather conditions.

3) *Mid-field, Low-Altitude Manual Guidance System:* the use of navigational, aircraft state, terrain database, forward sensor information, and pilot displays to present an above tree-top 3-dimensional, trajectory to the pilot for particular mission scenarios, using manual (pilot) control.

4) *Near-field, Pilot-Directed Automated Guidance System:* the use of aircraft state information, terrain database, forward sensors, and pilot displays to provide a below tree-top (NOE) trajectory to the pilot, providing automatic control maneuvers in the event of a potential ground or obstacle collision.

The paper will describe the results of the NASA ANOE program in the above technical component areas, summarize the programs findings, and provide future program directions.

OVERALL ANOE SYSTEM ARCHITECTURE

The complete automated NOE system draws on a terrain / obstacle database in generating trajectory guidance, which is presented to the pilot through helmet-mounted displays. Maneuvering the aircraft along the recommended trajectory is directed by the pilot, although assisted through automatic control. At his discretion, the pilot may elect to delegate complete maneuvering control of the aircraft to the automatic system. It is unlikely, however, that such fully automatic operation will constitute typical operations, as pilots are justifiably unwilling to relinquish such total authority to any automatic system. Our proposed automated NOE system architecture is shown as Fig. 1.

A combination of forward sensors and digitized terrain elevation maps is necessary to provide the required far, mid, and near-field planning [1, 2]. "Far-field" or mission planning yields course waypoints of several miles apart and takes into account mission requirements and global threat information. Existing mission or route planners, drawing from relatively course digitized terrain maps, are sufficient for such purpose [3, 4]. A high resolution digital map, such as those commonly available by the U.S. Defense Mapping Agency (~100m resolution) [5] is required to provide mid-field trajectory planning. Such maps allow a low-altitude, short duration (~1 minute), "mid-field" valley-seeking guidance trajectory to generated and refine the far-field route [6]. Such valley-seeking, lateral and vertical maneuvering flight is commonly termed terrain following / terrain avoidance (TF/TA) flight.

The complement of non-energy emitting passive sensors, such as visible-band cameras or forward-looking infrared (FLIR), and those that actively emit energy, e.g. radar and laser radar, are necessary for "near-field" planning. Near-field planning adjusts the mid-field guidance trajectory with regard to unmapped or unknown obstacles, such as trees, wires, and structures. Most digitized terrain maps do not record such obstacles, and those that try cannot account for hazards placed after map sampling, a likely event even in non-hostile environments. These passive and active forward sensors update the digitized terrain maps with high resolution, high accuracy terrain and obstacle information which can then be used for close-in, near-field obstacle avoidance.

Passive sensors, which use the parallax between a sequence of images to obtain ranging to obstacles, have the advantages of high update rates, wide field of views, and, in the military NOE application, covertness. They are limited in degraded weather operation, however, and typically produce sparsely populated, non-uniform obstacle maps. Their resolution is also not fine enough for wire detection. Active sensors, such as millimeter-wave (MMW) radar or laser radar (ladar), provide much denser, more uniform obstacle maps through monitoring of electromagnetic emissions and returns. MMW radar affords operation in degraded weather, while ladar (and possibly some radar bands) can offer wire detection. Active sensors typically provide relatively low update rates for comparable fields of view to passive sensors. As such, both types of complementary sensors are required for realizing near-field obstacle detection and avoidance.

The full-mission guidance is the result of the far-field mission planning guidance, mid-field low-altitude TF/TA guidance, and that of the near-field obstacle avoidance guidance. This guidance is then presented to the pilot through a pilot-centered full-mission display. This display includes modes for low-altitude TF/TA operations and for NOE operations. Such displays are intimately coupled with the degree of control allotted to the automatic system. The level of automation and associated pilot interface strongly influence pilot acceptability, which is crucial to the realistic success of an automated NOE system.

ANOE PROGRAM COMPONENT TECHNOLOGIES

PASSIVE SENSORS

Electro-optical sensors, such as visible- and infrared-band cameras, offer their wide field-of-view and fast update rate as advantages for obstacle detection and ranging applications without the need for radiating energy into the environment. Earlier systems utilizing these sensors relied on extensive a priori knowledge of the objects to be detected and/or interaction with a human user to designate the objects of interest. In the NOE application where the role of the sensors is to detect unexpected objects (i.e., those not appearing in digital terrain maps) and to aid in reducing the pilot's workload, neither of these assumptions apply. In addition, the sensor must fulfill the additional role of determining the position of detected obstacles.

Fig. 2. RASCAL helicopter with stereo cameras (outboard) and infrared camera (center) during data collection flights.

Approach: Beginning in 1986, the theoretical foundation for the obstacle detection and ranging algorithms were established [7]. Given the ability to measure the motion of an object between frames in an image sequence and measurements of the camera's motion state, a Kalman filter was developed to estimate the object's position (range, azimuth, and elevation) under the assumption that the object is not moving. This approach allows for detection and ranging under the full 6 degree-of-freedom maneuvering expected during NOE operations.

Implementation and Recorded Flight Test Data Results: Following initial laboratory demonstrations and testing [8-10], flight test data were collected to support development and validation of the single-camera obstacle detection and passive range estimation algorithms. A single monochrome camera was mounted in the nose of a CH-47 Chinook helicopter. Aircraft state information was measured using an inertial navigation system (INS). Truth measurements of obstacle positions relative to the helicopter were obtained using a ground-based laser tracking system. Off-line results using these flight data demonstrated the ability to detect objects at a distance of up to 700 feet and to estimate range within 10 percent error by the time the helicopter had travelled one-tenth the distance toward the object [11].

The initial approach was expanded to incorporate multiple cameras to overcame limitations in ranging to objects directly along the helicopter's path [12]. In addition, enhancements to the range-estimation filter resulted in an improved capability for ranging to distant objects [13]. Development of the multi-camera ranging algorithms led to a follow-on flight test in which two cameras were mounted

Fig. 3. Truck obstacles parked on runway during final approach landing sequence.

one meter apart on the nose of a UH-60 Blackhawk helicopter. Figure 2 portraits the NASA/Army RASCAL test helicopter [15] equipped with stereo outboard visible-band cameras and infrared centerline camera. A Litton LN-93 INS and an Ashtech differential GPS system provided the aircraft state information. As before, a ground-based laser tracker was used to measure the true obstacle positions for validation of the passive ranging algorithms. Analysis of the resulting data showed improved range accuracy and an extended range to 1000 feet [14]. A summary of passive ranging results obtained from flight test is provided in Fig. 3 and Table 1. In the flight test scenario recorded, several trucks were parked on a runway during a 3 deg glide-slope landing.

To extend the obstacle detection and passive ranging capability in support of night operations, NASA in conjunction with the U.S. Air Force Wright Laboratory conducted an additional flight test using a 3-5 micron focal plane array infrared camera. Under a joint agreement, Wright Lab supplied a FLIR Systems Prism camera which was installed on the nose of the UH-60. A bore-sighted monochrome video camera was synchronized with the IR camera and mounted next to the IR camera with a separation of approximately 4.5 inches. Flights were conducted at night and in poor visibility conditions (light rain, fog, and haze).

Having validated through flight data the feasibility of obstacle detection using passive sensors, our focus shifted to achieving real-time operation. An estimated 2 billion floating point operations per second were required to achieve real-time performance of the multi-camera algorithm at a rate 15 frame-pairs per second. Since this computational requirement is beyond the capability of off-the-shelf

Table 1. Summary of passive ranging results given imaging sequence of Fig. 3.

Truck	Frame	Truth Range (ft)	Monocular Range (ft)	Motion/Stereo Range (ft)
A	1	488	171	489
	60	399	405	431
	120	316	335	350
	180	235	227	247
B	1	614	270	785
	60	525	568	587
	120	443	462	463
	180	363	364	341
C	1	741	267	739
	60	650	519	498
	120	568	606	565
	180	487	514	486
D	1	860	138	n/a
	60	770	618	594
	120	688	653	799
	180	609	534	671
E	1	991	122	955
	60	899	995	813
	120	817	594	698
	180	736	863	722

microprocessors and digital signal processors, parallel processing technology was employed. The selection of a parallel processing architecture addressed trade-offs in overall speed increase, processor utilization, programmability, and physical constraints. In addition, a promising system needed to be adaptable to changes in the vision algorithm, exhibit good scalability, and be able to be installed on board a helicopter. Several multi-processor architectures were investigated, including a traditional image processing architecture, a shared-memory system, and two distributed-memory machines [16-20]. The most promising architecture, a distributed-memory multi-processor machine, was successfully implemented under a Small Business Innovative Research (SBIR) contract awarded to Innovative Configurations, Inc. The resulting system utilizes 32 Intel i860 processors and a stereo image acquisition system implemented on three 9U VME computer boards to detect and range to 300 "objects" at an update rate of 15 Hz. An object in this context is defined as an entity trackable through passive ranging algorithms, such as a physical object's edge or corner. The truck obstacles of Fig. 3 commonly provided several dozen such objects for tracking.

Following laboratory testing, the real-time passive ranging system is planned to be modified for airborne operation and installed on board the NASA/Army UH-60 RASCAL helicopter for flight demonstration. The system will obtain all required inputs directly from aircraft sensors for demonstration of real-time passive ranging capability at low altitude under full 6 degree-of-freedom maneuvering.

ACTIVE SENSORS

Active sensors offer the ability to operate in degraded weather with precise ranging measurements, but at slower update rates for comparable field of views to passive sensors, The millimeter-wave (MMW) band allows for relatively small antennas and narrow beam shapes, which, if configured as a "pencil-beam" 3-d radar, provides precise range, azimuth, and elevation to obstacles and terrain. This allows great flexibility in implementation and use of the radar information beyond that required for the near-field guidance planning of ANOE flight.

Approach: The scanning, pencil-beam MMW radar allows a terrain and obstacle database (TOD) to be constructed and presented to the pilot as a synthetic perspective display. It also drives an alternate display of a guidance trajectory with obstacle avoidance capability. The synthetic perspective display would be of greatest benefit during flight operations in unfamiliar areas, such as those encountered during heli-borne emergency medical service (EMS), search and rescue, and airborne fire-fighting missions. The obstacle sensitive guidance display would be of assistance during all phases of degraded weather operation.

Implementation: NASA is working jointly with Honeywell in developing a 35 GHz pulsed radar system for use in the NASA ANOE program and for use as a separate collision protection and warning device. The NASA/Honeywell 35 GHz bi-phase modulated, coherent pulsed MMW radar system takes advantage of existing 4.3 GHz radar altimeter components in performing the transmit and receive functions. The 4.3 GHz signal is passed through an upconverter to 35 GHz, and emitted as a scanning, pencil-beam through a twist-reflector type antenna. Radar returns are down-converted to 4.3 GHz and processed using the 4.3 GHz radar altimeter components. The use of 35 GHz affords good weather penetration capability, scattering at low grazing angles, and the use of a rather small antenna (11.8 in diameter).

The approximately 2.6 deg pencil-beams are scanned to cover a 20 deg elevation by 50 deg (azimuth) field of view (FOV) in 1 sec (fully interlaced in 2 sec). Range gating varies from 16 to 32 ft over the 1000 ft range of the radar. The radar system was designed to allow easy growth in range to 10,000 ft. An early single-beam, non-scanning version of this radar demonstrated excellent correlation between predicted and flight test performance [21].

The radar-derived TOD is presented to the pilot on a panel-mounted display as a 3-dimensional synthetic perspective "grid" display. Each grid is drawn at the height estimated from current and prior radar returns, and any stored map data that may be available. For engineering development, the grid perspective display can be overlaid onto a video image provided by a camera mounted adjacent to the radar.

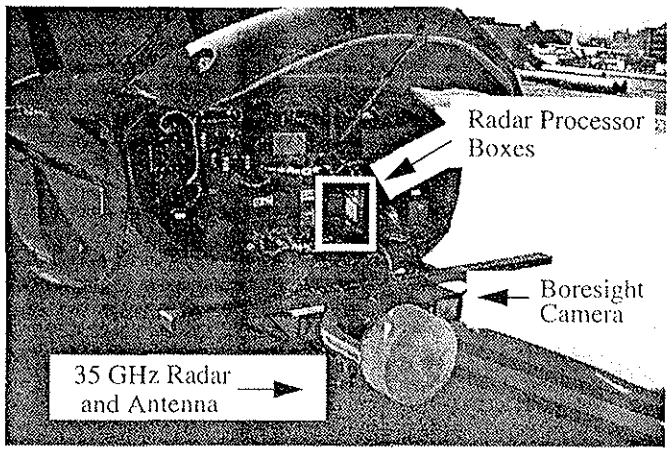

Fig. 4. RASCAL helicopter with NASA/Honeywell 35 GHz MMW radar.

An obstacle sensitive guidance trajectory can be generated using the radar-derived terrain and obstacle database. A flight plan is first entered, describing a route between several waypoints, desired MSL altitude, and minimum AGL altitude. A nominal straight-line course is then generated, and presented symbolically to the pilot on a panel-mounted display. The course is altered in elevation, however, should the minimum AGL altitude limit be breached, as determined through querying of the radar-derived database. The guidance trajectory is presented to the pilot in a "highway-in-the-sky" display format. Such a display has been extensively flight tested through a NASA/Army low-altitude flight guidance program [22]. This display will be described in the following section on mid-field, low-altitude manual guidance.

Early Flight Test Results: Flights are currently being conducted with the NASA/Honeywell 35 GHz radar aboard a NASA/Army UH-60 test helicopter based at Ames Research Center. This research aircraft includes GPS/INS navigation, digital data recorders for full aircraft state information (and radar outputs), and an externally mounted color camera. The 35 GHz radar is mounted on the nose of the aircraft on an experimental mounting bar (Fig. 4). A camera, mounted adjacent to the radar, allows merged video recordings of the pilot presentations of the perspective grid display or the "highway-in-the-sky" guidance display with that from the camera. The flight test course includes man-made obstacles (towers, buildings) and natural obstacles (trees, aggressive mountainous terrain, flat terrain) hazards. Data collected includes radar output, aircraft state, and pilot comments. Early flight test results have demonstrated the ability of the radar to reliably detect obstacles and generate a terrain / obstacle database from these radar detections [23].

MID-FIELD, LOW-ALTITUDE MANUAL GUIDANCE SYSTEM

A mid-field low-altitude terrain following / terrain avoidance (TF/TA) guidance system relying on digitized terrain elevation maps was developed that employs airborne navigation, mission requirements, aircraft performance limits, and radar altimeter returns to generate in real-time a valley-seeking, low-altitude trajectory between waypoints. Recall that "mid-field" refers to planning of approximately 1 min ahead and low-altitude is taken as no lower than tree-top altitude. By applying a cost function over an intended route between waypoints, a three-dimensional TF/TA route may be calculated in real-time.

Approach: The trajectory generation algorithm maintains a cost function that seeks to minimize mean sea level (MSL) altitude, heading change from a straight line nominal path between waypoints, and lateral offset from the nominal path. The cost function is applied to candidate trajectories from the current aircraft position over discrete pitch and roll angles. The lowest cost function trajectory (for the next 30 s) is then selected [4]. Adjusting constants of the cost function allows varying degrees of weighting to be applied to each performance criterion. The pilot selects aircraft performance limits and constants for the system. These include maximum bank, climb and dive angles, normal load factor, and desired velocity and set clearance altitude. Set clearance altitude is that AGL altitude to which the guidance algorithm will nominally seek. By severely penalizing, for example, those trajectories that deviate from the straight line nominal course (in heading and position), a straight line contour trajectory is generated. Such flight exclusively in the vertical plane is termed terrain following (TF) flight. Decreasing the penalty on these same two parameters allows lateral movement, and yields a meandering terrain following / terrain avoidance (TF/TA) flight profile. A general far-field flight plan, consisting of a series of course waypoints, is supplied by a mission planner or simply input by the crew, and can be changed in flight. The mission planner, if supplied with ground based threat information, will choose course waypoints sensitive to these hazards.

Implementation: The trajectory generated by the guidance system is presented symbolically to the pilot through a helmet mounted display (HMD). A simplified pictorial of the "pathway-in-the-sky" pilot presentation symbology on the head-tracked HMD is shown as Fig. 5, which presents a climbing left turn trajectory. The pathway troughs and phantom aircraft are drawn in inertial space along the desired trajectory. The troughs are 100 ft (30.5 m) wide at the base, 50 ft (15.2 m) tall, and 200 ft (61.0 m) wide at top, and are drawn in 1 sec increments of the trajectory out to 8 s, based on the aircraft's airspeed. The top center of each pathway is the desired, computed trajectory. The phantom aircraft flies

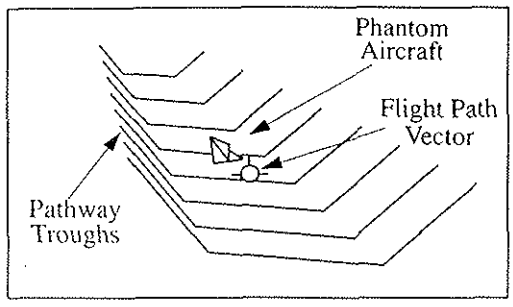

Fig. 5. Mid-field, low-altitude manual guidance system pilot symbology.

at the top center of the forth trough (the desired trajectory 4 s in the future). The aircraft's flight path vector is also drawn on the helmet mounted display, as predicted 4 s ahead. Hence, by tracking the phantom aircraft with the flight path vector, the pilot attempts to fly the desired TF/TA guidance trajectory. Additional aircraft state information also displayed (but not shown on Fig. 5) includes magnetic heading, engine torque, airspeed, radar altimeter, and ball and slip indicator. A horizon line, pitch ladder, and aircraft nose chevrons are also given to improve situational awareness. An airspeed flight director tape reflects deviation from the pilot selected, desired airspeed. This symbology set was developed over several piloted, motion-based simulations with a diverse group of pilots, and gives good trajectory tracking performance with low pilot workload. Such a "pilot-centered" display, providing trajectory lead information and heightened situational awareness, is preferred by pilots to traditional "flight-director" ILS-type displays [24].

Piloted Simulation and Flight Test Results: The TF/TA guidance system evolved through four motion-based, piloted simulations on the NASA Ames Vertical Motion Simulator (VMS) facility. These simulations served to develop the guidance algorithm, pilot display laws, and pilot display symbology, and included studies of individual display elements, pilot handling qualities ratings, and pilot workload. The TF/TA guidance system was then implemented for flight evaluation with the U.S. Army Command/Control Systems Integration Directorate (C2SID), Ft. Monmouth, NJ, aboard their NUH-60 STAR (Systems Testbed for Avionics Research) helicopter, through a Memorandum of Agreement.

The guidance system was further validated through flight test and supporting VMS simulations in three phases: 1) the baseline terrain map-based system, 2) the radar altimeter Kalman filter system, and 3) the forward sensor equipped system, which added an obstacle avoidance capability. The phases built upon one another and progressively increased in complexity and capability (Fig. 6). The guidance system has been extensively flight tested in a variety of terrain, primarily rugged terrain in So. Central Pennsylvania. The baseline system's performance is

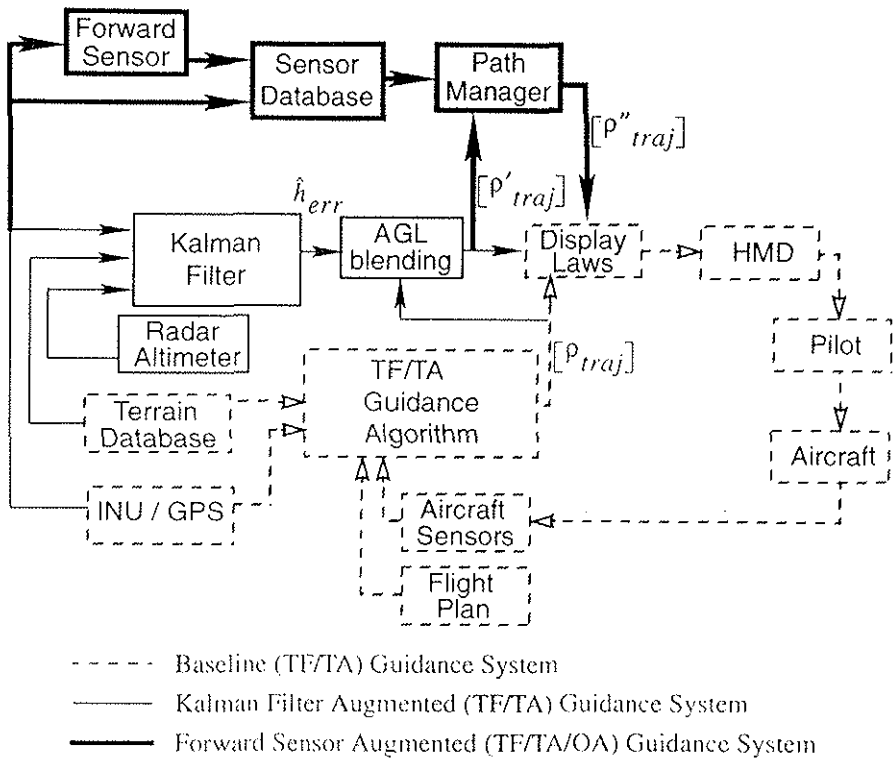

Fig. 6. Mid-field, low-altitude manual guidance system block diagram.

principally limited in its ability to position itself above the terrain, and its inability to detect and avoid unmapped obstacles, such as trees and wires. The above ground positioning limitation was found dominant and restricted flight to above 300 ft AGL at the operational design speeds between 80 and 110 kts [25].

The dashed blocks of Fig. 6 detail the extension to the baseline TF/TA guidance system resulting from a Kalman filter augmentation. The predicted AGL altitude, calculated as the difference in the navigation system MSL altitude and the stored map terrain elevation, together with the radar altimeter measurement, are blended in a Kalman filter to yield an estimate for the difference error from the predicted AGL altitude. This difference error value, $\hat{h}_{err}$, is then used to alter the terrain elevation database referenced guidance trajectory at the AGL-error blending block of Fig. 7. This modified trajectory is then presented to the pilot using the existing display laws and symbology. The enhancement produced trajectories more reflective of the topography and allowed for lower altitude operation than that of the baseline guidance system. The minimum flight altitude was reduced from 300 ft AGL altitude to 150 ft at operational speeds from 80 to 110 kts [26]. Flight restrictions for the terrain-referenced guidance system were now governed by pilot obstacle detection and avoidance, which could be assisted by a forward-looking sensor.

The forward sensor enhancement to the NASA/Army mid-field manual guidance system involved the addition of three distinct components; a wide field of view forward looking laser radar, a terrain/obstacle database generated from sensor returns, and a path manager, which modifies the guidance trajectory if necessary after querying the sensor database (Fig. 6).

The forward sensor integrated was the Northrop Obstacle Avoidance System (OASYS) laser radar prototype sensor developed by the U.S. Army [27, 28]. The terrain and obstacles located by the forward sensor are stored in an inertially-referenced square grid system periodically shifted such that its center position remains approximately below the aircraft. The database is updated with a group of OASYS detected "objects", nominally at 10 Hz. A "path manager" is used to alter the guidance trajectory in the event of an altitude clearance problem, as determined by the elevations of obstacles and terrain stored in the sensor generated database. All adjustments made to the trajectory are in vertical position only, i.e. no lateral modifications are made. Note that the optimization about the cost function described earlier for the guidance trajectory is not recomputed, i.e. this is not a "closed loop" forward sensor trajectory solution.

A representative flight test result from a terrain following (TF) mission is shown as Fig. 7. Terrain following flight, or contour flight, is flown at constant heading between

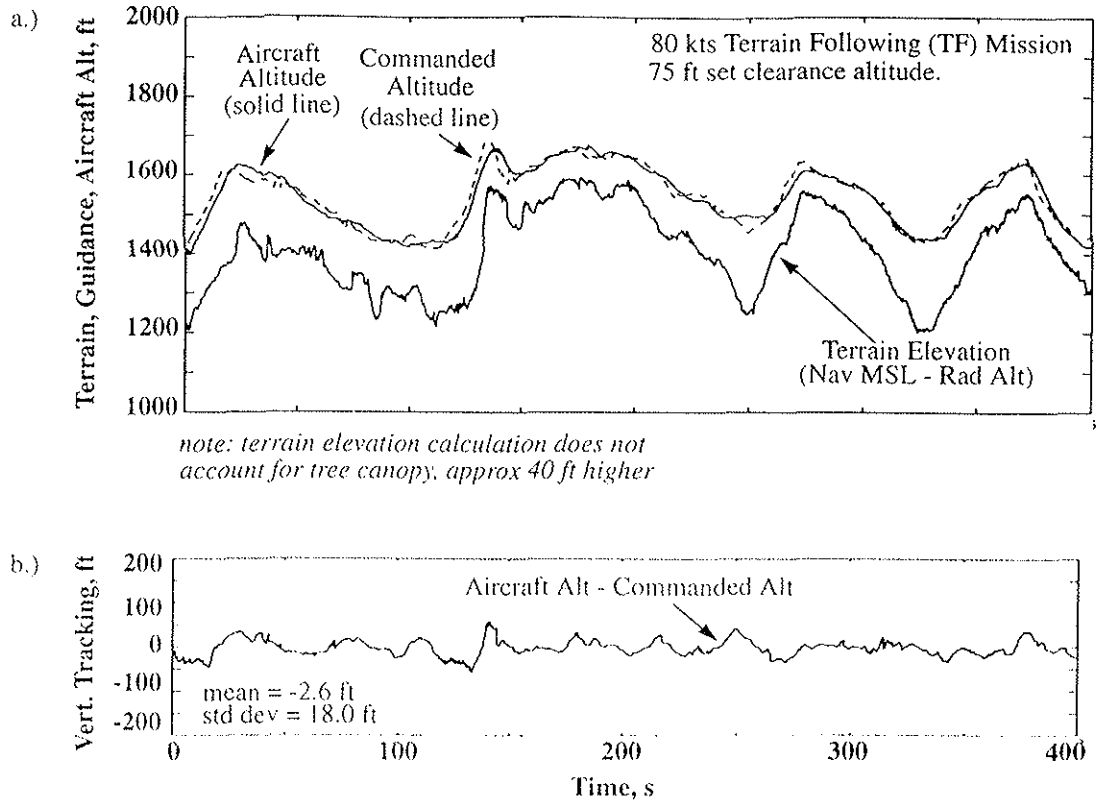

Fig. 7. Flight test results of low-altitude, manual guidance system.
a.) Elevation (vertical) profile.
b.) Pilot elevation tracking of guidance trajectory.

waypoints with only vertical maneuvering. The ground track of such flight results in straight lines between waypoints. This TF mission was flown at 80 kts airspeed and set clearance altitude of 75 ft, creating expected guidance trajectory AGL clearances of 75 ft AGL and above. These figures trace the elevation or vertical track (Fig. 7a), as well as the pilot's tracking of the guidance trajectory through the HMD symbology previously discussed (Fig. 7b). The upper solid line traces the aircraft MSL altitude while flying the forward-sensor equipped guidance system. The upper dashed line tracks the desired (or "commanded") trajectory MSL altitude, which is that computed by the trajectory algorithm as modified by the forward sensor dependent path manager and presented to the pilot. The difference between these two lines, representing the pilot's vertical tracking of the desired trajectory, is given as Fig. 7b. The lowest solid line of Fig. 7a is the "truth" measurement of the terrain elevation, which is calculated as the aircraft's MSL altitude minus the radar altimeter measurement.

The commanded (path manager corrected) pathway of Fig.7a presents a smooth but aggressive trajectory. Terrain undulations are clearly recognized and reflected in the pathway placement. Areas where the guidance pathway appears too high are most likely due to local foliage effects, i.e. a tight, higher concentration of trees, or the effect of the smooth flight path angle constraint imposed on all guidance trajectories. Figure 7b shows the difference between the elevation (vertical) command position and that of the aircraft. Mean elevation tracking was -2.6 ft, with standard deviation of 18.0 ft. Except for the period surrounding the hill just prior to time 150 s, tracking is within the trough vertical bounds of 50 ft. Imperfect trajectory tracking can be traced to two principle reasons: the pilot can never track the symbology perfectly, and at times will override the recommended pathway. Circumvention of the commanded trajectory occasionally occurs when a pilot "short-cuts" the suggested guidance trajectory, such as when a ridge is crossed followed by negative sloping terrain.

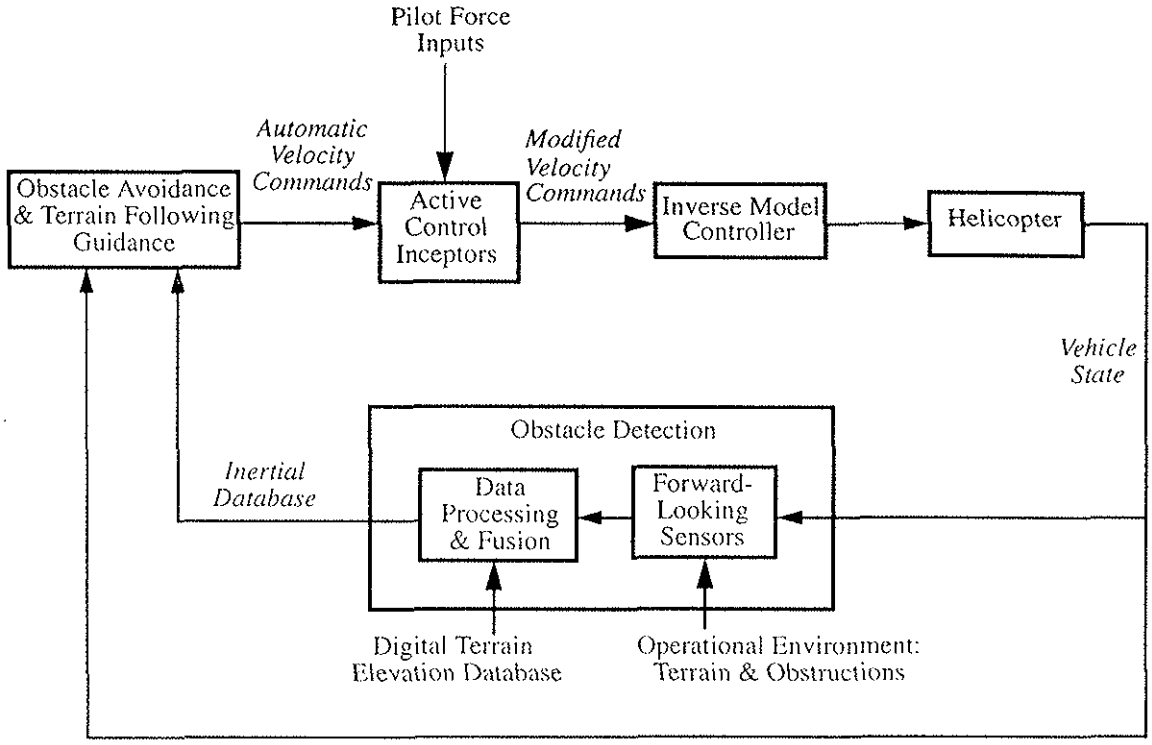

Fig. 8. Near-field, pilot-directed automated guidance system diagram.

NEAR-FIELD, PILOT-DIRECTED AUTOMATED GUIDANCE SYSTEM

Early efforts at NASA Ames Research Center to reduce pilot workload by automating tasks for NOE flight involved the development of a fully automatic obstacle avoidance system implemented in a real-time workstation based simulation. The technical emphasis of this effort was on the development of guidance and control laws that selected and followed open paths for safe maneuvering based upon the identification of terrain and obstacles from simulated onboard sensor information [29]. Resulting guidance commands were generated in the form of a 3-dimensional commanded velocity vector. The autopilot-controller, based upon an inversion of the vehicle dynamics, was responsible for computing the cyclic, collective, and rudder control inputs needed to follow the guidance command.

Approach: Following the development of the guidance and control functions for fully automatic flight, research efforts were directed towards the development of an effective means by which a human pilot could interface with the automated systems. The goal was to develop an interface that took advantage of the workload reduction potential of fully automatic guidance and control without compromising pilot confidence and mission flexibility. Qualitative results from previous simulation studies of automated NOE obstacle avoidance systems identified the pilot-interface as being the most crucial factor influencing pilot acceptability [30]. In particular, studies suggested that poor pilot acceptability would result from any waypoint following, fully automatic NOE system that required pilots to perform merely as system monitors.

Research aimed at identifying effective pilot interface solutions resulted in the selection of a concept referred to as Pilot-Directed Guidance (PDG). The PDG concept, shown schematically in Fig. 8, is based upon a translational velocity-command control system that provides continuous obstacle avoidance protection while depending upon the pilot for overall course guidance [31]. With this interface, a pilot can concentrate upon primary course guidance and secondary cockpit tasks by delegating obstacle detection and avoidance tasks to the PDG system. The PDG system assists pilots flying NOE by providing for 1) automated obstacle detection and avoidance, 2) terrain-following altitude control, and 3) airspeed control. PDG relies upon real-time forward-looking sensor information to provide the system with knowledge of obstacles and terrain in the vicinity of the rotorcraft. In the event that the PDG system determines that an obstacle or terrain collision will take place within the PDG look-ahead time window, the necessary avoidance control activity is provided automatically for the pilot. The PDG guidance logic is designed to favor lateral maneuvers over vertical maneuvers in order to provide greater

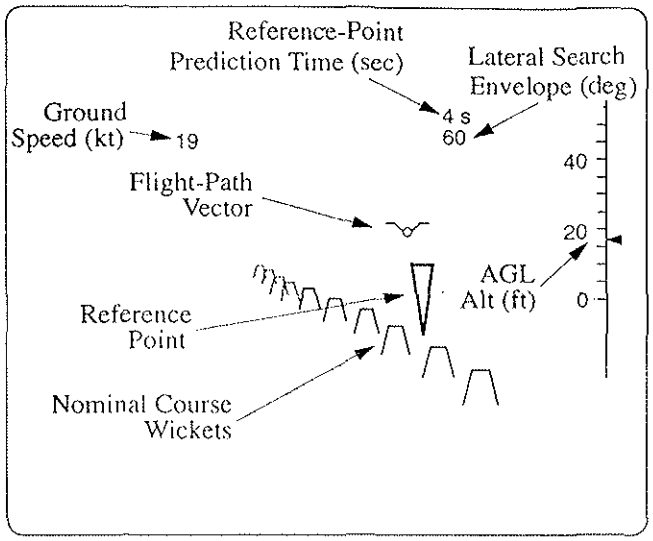

Fig. 9. Near-field, pilot-directed automated guidance system pilot symbology.

concealment of the vehicle under hostile conditions. Vertical maneuvers are executed by system in the event that all lateral maneuvering options have been exhausted.

Implementation: To improve situational awareness and PDG system monitoring, a Helmet-Mounted Display (HMD) is provided for the pilot. Along with rotorcraft and system state information, the HMD displays inertially referenced course-following symbology that resembles a path-way on the ground described by a series of symbols resembling croquet wickets, as shown in Fig. 9. This course symbology is similar to the pathway in the sky symbology used in the mid-field, low-altitude manual guidance system of the previous section except that the troughs are inverted and anchored to the ground. This provides a more meaningful visual reference to the pilot at very low NOE altitudes. The height of the wickets are set to the PDG commanded radar altitude to provide additional altitude tracking information to the pilot. A ground-based symbol representing the predicted position of the vehicle at the end of the PDG look-ahead time window is also displayed on the HMD. This symbol, referred to as the PDG reference point, resembles an inverted triangle that has its vertex in contact with the terrain surface and its height equal to the PDG commanded radar altitude [32]. Additional symbology provided, by not shown on Fig. 9, includes a horizon line, boresight indicator, heading indicator, and pitch reference. Automatic obstacle-avoidance control activity is executed whenever a direct line-of-sight to the PDG reference point is obstructed.

To provide a pilot cueing mechanism of automatic control activity, the cyclic and collective control inceptors are back-driven in the cockpit. The pilot is able to override the PDG system at any time by providing a sufficient force input to the control inceptors. The final control inceptor positions, governed by the pilot, are interpreted as the velocity command inputs that are sent to the high bandwidth autopilot controller.

The PDG controller is based upon a non-linear, feedback linearization design technique that facilitates its use over the entire flight envelope of the vehicle. The feedback linearization technique is used to transform the input-output map of the original nonlinear system into a linear time-invariant form [33]. The transformed system is then easily controlled using any well-known linear control design technique. Further simplification of the design process can be realized by dividing the rotorcraft dynamics into multiple time scales of reduced order using the singular perturbation method. The advantage of using this method is that the resulting controllers will also be of reduced order. A baseline nonlinear inverse autopilot design incorporating feedback linearization and time-scale separation was designed and synthesized for a comprehensive flight test validated engineering model of the UH-60A Black Hawk helicopter for the PDG application. The system uses a stored-trim-map approach to approximate the inverse force and moment model of the rotorcraft used during feedback linearization. A simple time-invariant PD type control law design is used throughout the operational flight envelope.

Piloted Simulation Results: The control laws of Fig. 8 along with the guidance in Fig. 9 were evaluated through piloted simulation in the NASA Ames six degree-of-freedom Vertical Motion Simulator (VMS). Results demonstrate the capability of the PDG automated system to significantly improve flight path performance and reduce pilot workload for NOE missions requiring obstacle avoidance. Flights were conducted both with and without PDG automation for direct comparison of flight path performance and pilot workload. An example of the NOE conditions encountered in the simulation are shown in Fig. 10 which shows an out-the-window view as seen by the pilot.

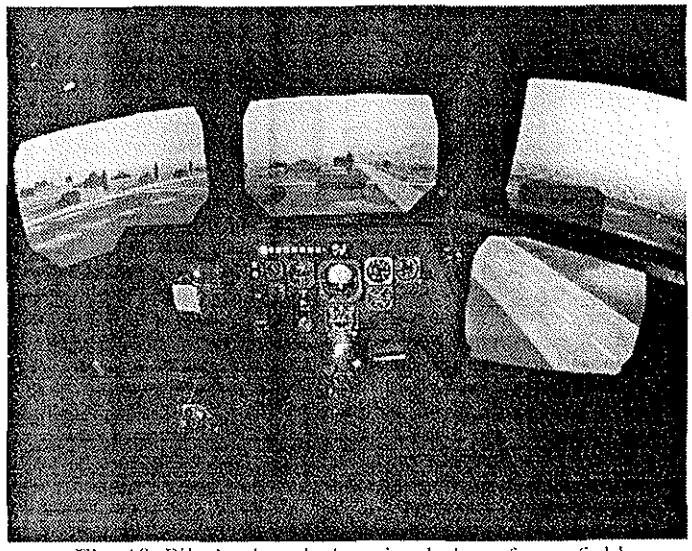

Fig. 10. Pilot's view during simulation of near-field, pilot-directed automated guidance system.

Under low visibility conditions, time exposed above tree level was reduced by 75% with the PDG system compared with that of non-automated flights. Increased obstacle clearances, leading to a reduction in obstacle strikes, were also observed with PDG. Secondary performance benefits, resulting from the PDG automation, were greatly improved airspeed and altitude command following. Most importantly, simulation evaluations have demonstrated the potential of the PDG system to substantially reduce overall pilot workload over a range of speed and visibility conditions [31].

CONCLUDING REMARKS

This paper summarizes the status and results to date of the NASA Automated Nap-of-the-Earth (ANOE) program. A structure involving sensor and database derived guidance, pilot-centered displays, and pilot-automatic control interaction has been employed. Results have been demonstrated through laboratory development, piloted, motion-based simulation, and through flight testing in the technology focus areas of passive sensors, active sensors, mid-field manual TF/TA guidance, and near-field pilot-directed automatic guidance.

Algorithms have been developed using calibrated flight test images and a specialized 32-board parallel processor computer that can perform ranging to objects from passive sensors in real-time. Ranging to 500 image objects at 15 Hz through visible-band or infrared cameras have achieved ranging accuracies of 5% of range given recorded flight test collected imaging data. Real-time operation has been laboratory demonstrated. Real-time in-flight demonstration of this capability aboard a test helicopter is on-going. Real-time passive ranging to objects has direct application in robotics, airport terminal area operations, and in planetary rovers. Work in passive ranging has supported the external vision component of the NASA high-speed research program, and is applicable to any synthetic-vision system. Calibrated flight test data sets have been distributed to numerous universities and government laboratories.

A scanning, pencil-beam millimeter-wave radar has been developed which can create a local, high-resolution database surrounding an aircraft for direct 3-dimensional perspective display or to drive higher-level guidance. Such an obstacle detection and avoidance capability has immediate value to commercial emergency medical service (EMS) operations, airborne fire-fighting, and reduced visibility operations. This MMW radar system and display have begun flight trials and have demonstrated their obstacle detection capability.

A mid-field, low-altitude manual guidance system has been developed and extensively flight tested in cooperation with the US Army. When augmented with a laser radar forward-sensor, low-altitude obstacle avoidance capable flights to 75 feet AGL at 80-110 kts have been achieved. Guidance trajectories, generated and then modified in real-time by forward-sensor obstacle detections, are presented to the pilot on a helmet-mounted display. This guidance system has direct application to the military and is now being employed in a U.S. Special Operations test program.

A near-field, pilot-directed automated NOE guidance system has been developed and is being refined through piloted, motion-based simulation. The system incorporates back-driven controls and a helmet-mounted display. The system retains principle and ultimate authority with the pilot while providing an automatic clobber protection capability. Under low visibility conditions, time exposed above tree level was reduced by 75% with this system compared with that of non-automated flights. Increased obstacle clearances, leading to a reduction in obstacle strikes, were also observed with the pilot-directed guidance system. Simulation evaluations have demonstrated the potential of this pilot-directed automated NOE guidance system to substantially reduce overall pilot workload over a range of speed and visibility conditions.

Future work will focus on the optimal merging of passive sensor and active sensor derived obstacle rangings in creating a local, high-resolution terrain and obstacle database. Work on pilot interaction with automated guidance through pilot-centered displays will continue. Eventual flight demonstration of an integrated automated NOE flight guidance system is conceivable within the coming years.

REFERENCES

[1] Cheng, V.H.L., and Sridhar, B., "Technologies for Automated Nap-of-the-Earth Flight," *Journal of the American Helicopter Society*, Vol.38, (2), April 1993.

[2] Cheng, V.H.L., and Sridhar, B., "Considerations for Automated Nap-of-the-Earth Flight," *Journal of the American Helicopter Society*, Vol. 36, (2), April 1991.

[3] Deutsch, O.L., Desai, M., and McGee, L.A., "Far-field Mission Planning for Nap-of-the-Earth Flight," *Proceedings of the AHS national Specialists Meeting on Flight Control and Avionics*, Cherry Hill, N.J., Oct. 1987.

[4] Pekelsma, N.J., "Optimal Guidance with Obstacle Avoidance for Nap-of-the-Earth Flight," NASA TM 177515, Dec. 1988.

[5] Babiak, N., "The Defense Mapping Agency and Tomorrow's Advanced Aerospace Warfare Systems," *Proceedings of the IEEE National Aerospace and Electronics Conference*, Inst. of Electrical and Electronics Engineers, New York, 1990, pp. 260-264.

[6] Denton, R.V., Pekelsma, N.J., Hagen, M., and McGee, L.A., "Guidance Automation for Nap-of-the-Earth Flight,"

Proceedings of the 7th Annual Digital Avionics Systems Conference, Fort Worth, TX, Oct. 1986, pp. 261-266.

[7] Sridhar, and Phatak, A., "Simulation and Analysis of Image-Based Navigation system for Rotorcraft Low-Altitude Flight," *Proceedings of the American Helicopter Society Specialists' Meeting on Automation Applications of Rotorcraft*, Atlanta, GA, April 1988; IEEE Transactions on Systems, Man and Cybernetics, vol. 22, no. 2, pp. 96-101, March/April 1992.

[8] Sridhar, B., Suorsa, R., and Hussien, B., "Passive Range Estimation for Rotorcraft Low-altitude Flight," NASA TM, October 1990.

[9] Suorsa, R. and Sridhar, B., "Validation of Vision Based Obstacle Detection Algorithms for Low Altitude Flight," *Proceedings of the SPIE International Symposium on Advances in Intelligent Systems*, Boston, MA, November 1990.

[10] Sridhar, B, Suorsa, R., and Smith, P., "Vision-based Techniques for Low Altitude Flight", *International Symposium on Intelligent Robotics*, Bangalore, India, Jan 1991.

[11] Smith, P.N., Sridhar, B., and Hussien, B., "Vision-Based Range Estimation Using Helicopter Flight Data," *Proceedings of the 1992 IEEE Computer Society Conference on Computer Vision and Pattern Recognition*, Champaign, Illinois, June 15-18, 1992; NASA TM 103930, June 1992.

[12] Sridhar, B. and Suorsa, R., "Integration of Motion and Stereo Sensors in Passive Ranging Systems," *IEEE Transactions on Aerospace and Electronic Systems*, vol. 27, No. 4, pp. 741-746, July 1991.

[13] Sridhar, B., Smith, P.N., Suorsa, R.E., and Hussien, B., "Multirate and Event Driven Kalman Filters for Helicopter Passive Ranging," *Proceedings of the 1st IEEE Conference on Control Applications*, Dayton, Ohio, September 1992.

[14] Smith, P.N, Sridhar, B., and Suorsa, R.E., "Multiple-Camera/Motion Stereoscopy for Range Estimation in Helicopter Flight," *Proceedings of the 1993 American Control Conference*, San Francisco, California, June 2-4, 1993.

[15] Jacobsen, R.A., Rediess, N.A., Hindson, W.A., Aiken, E.W., and Bivens, C.C., "Current and Planned Capabilities of the NASA/Army Rotorcraft Systems Concepts Airborne Laboratory (RASCAL)", *Proceedings of the American Helicopter Society 51st Annual Forum*, Ft. Worth, TX, May, 1995.

[16] Fong, T.W., and Suorsa, R.E., "Real-time Optical Flow Range Estimation on the iWarp," *Proceedings of the SPIE International Symposium on Intelligent Information Systems*, Orlando, Florida, April 1993.

[17] Suorsa, R.E., Sridhar, B., and Fong, T.W., "Real-Time Computational Needs of a Multisensor Feature-Based Range-Estimation Method," *Proceedings of the SPIE International Symposium on Optical Engineering and Photonics in Aerospace Science and Sensing: Sensor Fusion and Aerospace Applications*, Orlando, Florida, April 1993.

[18] Karmarkar, J.S., and Sridhar, B., and Lakshmanan, M., "Cost-effective Implementation of Passive Ranging Algorithms on General Purpose Parallel Architectures," *Proceedings of the SPIE International Symposium on Optical Engineering and Photonics in Aerospace Science and Sensing: Sensor Fusion and Aerospace Applications*, Orlando, Florida, April 1993.

[19] Suorsa, R.E., and Sridhar, B., "A Parallel Implementation of a Multisensor Feature-Based Range-Estimation Method," *Proceedings of the 1993 IEEE Computer Society Conference on Computer Vision and Pattern Recognition*, New York, New York, June 1993.

[20] Sridhar, B., and Suorsa, R.E., "Computer Architectures for a Real-time Passive Ranging Algorithm," *Proceedings of the IEEE/AIAA Digital Avionics Systems Conference*, Ft. Worth, 1993.

[21] Becker, Robert C., and Almsted, L.D., "Flight Test Evaluation of a 35 GHz Forward Looking Altimeter for Terrain Avoidance," *Proceedings of the IEEE/AIAA Digital Avionics Systems Conference*, Phoenix, 1994.

[22] Zelenka, R.E., Clark, R.F., and Branigan, R.G., "Flight Test of a Low-Altitude Helicopter Guidance System with Obstacle Avoidance Capability," NATO AGARD CP-563 Mission Systems Panel Symposium, Pratica di Mare (Rome), Italy, Oct. 25-27, 1994.

[23] Almsted, L.D., Becker, R.C., Zelenka, R.E., and Tucker, G.E., "Design and Preliminary Flight Test of a 35 GHz Forward-Looking Collision Avoidance Radar," *Proceedings of the American Helicopter Society 52nd Annual Forum*, Washington, D.C., June, 1996.

[24] Swenson, H.N., Zelenka, R.E., Hardy, G., and Dearing, M., "Simulation Evaluation of a Low-Altitude Helicopter Flight Guidance System," *Proceedings of the 10th IEEE/AIAA Digital Avionics Systems Conference* (Los Angeles, CA), 1991.

[25] Swenson, H.N., Jones, R.D., and Clark, R.F.; "Flight Evaluation of a Computer Aided Low-Altitude Helicopter Flight Guidance System," NATO AGARD CP-520 Flight Mechanics and Guidance and Control Panel Symposium, Edinburgh, UK, Oct. 19-22, 1992.

[26] Zelenka, R.E., Yee, Z., and Zirkler, A., "Flight Test of a Radar Altimeter Enhancement for Terrain-Referenced Guidance," *AIAA Journal of Guidance, Control, and Dynamics*, Vol. 18, No. 4, 1995, pp. 702 - 708.

[27] Branigan, R., "Design Requirements for an Obstacle Avoidance System (OASYS)," U.S. Army CNVEO Report, July 1992.

[28] Holder, S., and Dillon, R., "Army Helicopter Obstacle Avoidance System (OASYS): Performance Modeling and Preliminary Performance Data," *Proceedings, IRIS Specialty Group on Active Systems*, Oct., 1992.

[29] Cheng, V.H.L. "Concept Development of Automatic Guidance & Control for Helicopter Obstacle Avoidance," *Proceedings of the IEEE International Conference on Robotics and Automation*, Nice, France, pp. 252-260, May 1-12, 1992.

[30] Coppenbarger, R.A., and Cheng, V.H.L., "Concepts for Pilot Interaction with an Automated NOE Obstacle Avoidance System," *Proceedings of the AIAA Guidance, Navigation, and Control Conference*, Hilton Head Island, SC, Aug. 10-12, 1992.

[31] Coppenbarger, R.A., and Cheng, V.H.L., "Simulation of an Automated Rotorcraft Obstacle Avoidance System with Pilot Interface," *Proceedings of the American Helicopter Society National Specialists Meeting*, Fairfield County, CT, Oct. 6-7, 1993.

[32] Coppenbarger, R.A., "Helmet-Mounted Display Symbology for Automated Nap-of-the-Earth Rotorcraft Flight," *Proceedings of the SPIE Conference on Helmet-and Head-Mounted Display & Symbology Requirements*, Orlando, FL, April 5-7, 1994.

[33] Njaka, C.E., Menon, P.K., and Cheng, V.H.L., "Towards an Advanced Nonlinear Rotorcraft Flight Control System Design," *Proceedings of the IEEE/AIAA Digital Avionics Systems Conference*, Phoenix, 1994, pp. 190 - 197.